MCP Papers in Press. Published on June 23, 2014 as Manuscript M114.039446



# REDOX-STATE OF PENTRAXIN 3 AS A NOVEL BIOMARKER FOR RESOLUTION OF INFLAMMATION AND SURVIVAL IN SEPSIS

Friederike Cuello[1,2,3], Manu Shankar-Hari[4,5], Ursula Mayr[1], Xiaoke Yin[1], Melanie Marshall[1], Gonca Suna[1], Peter Willeit[6,7], Sarah R. Langley[1], Tamani Jayawardhana[1], Tanja Zeller[3,8], Marius Terblanche[4], Ajay M. Shah[1], Manuel Mayr[1]*

[1] King's British Heart Foundation Centre, King's College London, UK

[2] Department of Experimental Pharmacology and Toxicology, Cardiovascular Research Centre, University Medical Center Hamburg-Eppendorf, Hamburg, Germany

[3] DZHK (German Center for Cardiovascular Research), partner site Hamburg/Kiel/Lübeck, Germany

[4] Critical Care Medicine, Guy`s and St Thomas` NHS Foundation Trust, London, UK

[5] Division of Asthma Allergy and Lung Biology, King's College, London

[6] Department of Public Health and Primary Care, University of Cambridge, UK

[7] Department of Neurology, Innsbruck Medical University, Austria

[8] Clinic for General and Interventional Cardiology, University Heart Centre Hamburg, Hamburg, Germany

**Short Title:** Oligomerization of pentraxin 3 in sepsis

* To whom correspondence should be addressed: Prof. Manuel Mayr, King's British Heart Foundation Centre, King's College London, 125 Coldharbour Lane, London SE5 9NU, UK; Fax: +44 (0)20 7848 5296; ☎+44 (0)20 7848 5132; E-mail: manuel.mayr@kcl.ac.uk



Copyright 2014 by The American Society for Biochemistry and Molecular Biology, Inc.

**ABSTRACT**

In an endotoxaemic mouse model of sepsis, a tissue-based proteomics approach for biomarker discovery identified long pentraxin 3 (PTX3) as the lead candidate for inflamed myocardium. When the redox-sensitive oligomerization state of PTX3 was further investigated, PTX3 accumulated as an octamer due to disulphide-bond formation in heart, kidney and lung – common organ dysfunctions seen in patients with sepsis. Oligomeric moieties of PTX3 were also detectable in the circulation. The oligomerization state of PTX3 was quantified over the first 11 days in critically ill adult patients with sepsis. On admission day, there was no difference in the oligomerization-state of PTX3 between survivors and non-survivors. From day 2 onwards, the conversion of octameric to monomeric PTX3 was consistently associated with a greater survival after 28 days of follow-up. For example, by day 2 post admission, octameric PTX3 was barely detectable in survivors, but still constituted more than half of total PTX3 in non-survivors ($P<0.001$). Monomeric PTX3 was inversely associated with cardiac damage markers NT-proBNP, high sensitivity troponin I and T. In comparison to the conventional measurements of total PTX3 or NT-proBNP, the oligomerization of PTX3 was a superior predictor of disease outcome.

**ABBREVIATIONS:**

AOF, acute organ failure

AUROC, the area under the ROC curve

CRP, C-reactive protein

ELISA, enzyme-linked immunosorbent assays

hsTnI, high sensitivity troponin I

hsTnT, high sensitivity troponin T

ICU, intensive care unit

LC, liquid chromatography

LPS, lipopolysaccharide

LTQ, linear trap quadrupole

MS/MS, tandem MS

NT-proBNP, N-terminal of the prohormone brain natriuretic peptide

PTX3, long pentraxin 3

ROC, receiver operating characteristic

SOFA, sequential organ failure assessment

## INTRODUCTION

Severe sepsis is a common acute illness in intensive care units (ICU) with high mortality rates and chronic morbidity. When associated with hypotension (termed septic shock) mortality rate is very high (50-80%). Cardiovascular dysfunction during sepsis is multifactorial and often associated with minimal loss of myocardial tissue, but with release of myocardial specific markers like troponins. A key unmet clinical need is the availability of a biomarker that predicts myocardial dysfunction early, monitors response to treatment and thus identifies a cohort of patients at higher risk of septic shock to aid in targeted interventions and improve outcome (1).

In the present study, we use proteomics for biomarker discovery. Over the past decade, the field of proteomics has made impressive progress. Plasma and serum, however, are the most complex proteomes of the human body (2) and less abundant proteins tend to be missed in untargeted proteomics analysis of body fluids (3). Thus, we pursued an alternative strategy: the application of proteomics to diseased tissue (4), where the potential biomarkers are less dilute and their cellular origin is less uncertain (5-7). We employed a solubility-based, protein subfractionation methodology to analyze inflammatory proteins that are retained with sepsis tissue. This innovative proteomics approach shall reveal inflammatory molecules that reside and persist within the inflamed tissue. We hypothesized that proteins, which accumulate in the susceptible tissues are more likely to be biomarker candidates for organ dysfunction than proteins that just circulate in plasma or serum. Validation of our proteomics findings in the preclinical model was then performed using samples from sepsis patients admitted to ICUs.

## EXPERIMENTAL PROCEDURES

*Materials* – Antibodies recognizing pentraxin 3 (PTX3) were from Epitomics (now Abcam), α-actinin was from Sigma, cardiac myosin binding-protein C (cMyBP-C) was a kind gift from Prof. Mathias Gautel from King`s College London, telethonin was from Santa Cruz Biotechnology, GAPDH conjugated to horseradish peroxidase (HRP) was from Abcam. All other chemicals were from Calbiochem, Invitrogen, Sigma-Aldrich or VWR International, unless otherwise stated. Male C57BL/6J mice were obtained from B&K Universal Ltd.

*Animal models* – All experiments were performed in accordance with UK Home Office regulations and the investigation conforms with the Guide for the Care and Use of Laboratory Animals published by the US National Institutes of Health (NIH Publication No. 85-23 revised 1996). The mouse model employed in this study was one of moderate severity endotoxemia and has been characterised in detail previously (8, 9). In this model, there is significant hypotension with an approximately 25-30% decrease in systolic blood pressure at 12-18h after LPS injection. This is associated with significant cardiac dysfunction as assessed by *in vivo* volume loading protocols (8) or by *ex vivo* cardiac myocyte contraction (9). Mortality is approximately 10% at this stage. C57/BL6 mice were injected intraperitoneal (i.p.) with 9mg/kg *E. coli* bacterial lipopolysaccharide (LPS; serotype 0.11:B4, Sigma Aldrich, UK). Control animals received i.p. injections with an equivalent volume of saline. Mice were sacrificed 6-8 or 16-18h later after injection (9). Proteomics was performed 16-18h post injection, immunoblot analysis was performed both at an early (6-8h) and at a late time point (16-18h).

*Immunohistochemical analysis* – Tissue was post-fixed in 4 % formaldehyde, processed to paraffin blocks using an ASP300S dehydration machine (Leica, Wetzlar, Germany) and an EG1160 tissue embedding system (Leica, Wetzlar, Germany), and cut into 4 µm thick slices. Sections were stained using the Ventana Benchmark XT machine (Ventana, Tuscon, Arizona, USA). Deparaffinised sections were incubated for 60 min in CC1 solution (Ventana, Tuscon, Arizona, USA) for antigen retrieval. Primary antibodies were diluted in 5 % goat serum (Dianova), 45 % Tris-buffered saline pH 7.6 and 0.1 % Triton X-100 in antibody diluent solution (Zytomed, Berlin, Germany). Sections were then incubated with primary antibody against Iba1 (Wako Chemicals, USA, 1:2000), Ly6G (eBiosciences, 1:2000) or PTX3 (TNFAIP5 polyclonal, HRP conjugated, 1:100) for 60 min. Histofine Simple Stain MAX PO Universal immunoperoxidase polymer purchased from Nichirei Biosciences (Wedel, Germany) were used as secondary antibody. Detection of secondary antibodies was performed with an ultraview universal DAB detection kit from Ventana. Counterstaining was performed by using Ventana's hematoxylin solution. Sections were cover-slipped using TissueTek glove mounting medium (Sakura Finetek, Staufen, Germany), and dried in an incubator at 60°C.

*Subfractionation of mouse hearts* – Mouse heart homogenates were subfractionated into Triton-soluble and Triton-insoluble fractions. Briefly, 1% (v/v) Triton X-100 was added to the mouse heart homogenates and incubated for 15 min on a shaking platform at 4°C and centrifuged at 13,000g for 5 min (4°C). The Triton-soluble fraction was separated from the Triton-insoluble fraction, and non-reducing Laemmli sample buffer was added.

*Proteomics analysis* – The Triton-insoluble fractions from control (n=4) and septic group (n=4) were denatured in Laemmli buffer at 97°C for 5min. The proteins were separated by 5-20% gradient Tris-glycine gel at 5W for 45min then 30W for 4.5 h. After electrophoresis, gels were stained using the PlusOne Silver staining Kit (GE Healthcare). Silver staining was used for band staining to avoid cross-contamination with fainter gel bands. All gel bands (n=48 per sample) were excised in identical parallel positions across lanes and no empty gel pieces were left behind. Subsequently, all gel bands were subjected to in-gel tryptic digestion using an Investigator ProGest (Digilab) robotic digestion system. Tryptic peptides were separated on a nanoflow LC system (Dionex Ultimate 3000, Thermo Fisher Scientific) using reversed phase columns (PepMap C18, 25cm x 75um) and eluted with a 40min gradient (10-25% B in 35 min, 25-40% B in 5min, 90% B in 10min, and 2% B in 20min, where A is 2% ACN, 0.1% formic acid in HPLC $H_2O$ and B is 90% ACN, 0.1% formic acid in HPLC $H_2O$). Sequentially eluted peptides were directly analysed by tandem mass spectrometry (LTQ Orbitrap XL, Thermo Fisher Scientific) using full ion scan mode over the mass-to-charge (m/z) range 450-1600. Tandem MS (MS/MS) was performed on the top 6 ions using data-dependent mode with dynamic exclusion (10, 11). Peak lists were generated by extract_msn_com.exe (version 5.0, Thermo Fisher Scientific) and searched against UniProt/SwissProt mouse database (version 2014_01, 16656 protein entries) using Mascot (version 2.3.01, Matrix Science). The mass tolerance was set at 30ppm for the precursor ions and at 0.8 Da for fragment ions. Carboxyamidomethylation of cysteine was used as a fixed modification and oxidation of methionine as a variable modification. Two

missed cleavages were allowed. Scaffold (version 4.3.0, Proteome Software Inc., Portland, OR) was used to calculate the normalized spectral counts and to validate peptide and protein identifications. According to the default values in the Scaffold software, peptide identifications were accepted if they could be established at greater than 95% probability as specified by the Peptide Prophet algorithm. Only tryptic peptides were included in the analysis. Protein identifications were accepted if they could be established at greater than 99% probability with at least two independent peptides.

*Proteomic differential expression analysis* – Proteomic differential expression was assessed using the normalized spectral abundance factor - power law global error model (NSAF-PLGEM) (12). The Normalized Spectral Abundance Factor was calculated for each protein detected. Spectral count values of 0 were replaced by an empirically derived fractional value. The value was calculated to be the smallest value between 0 and 1, which provided the best fit to a normal distribution, as determined by a Shapiro-Wilks test. The NASF values were fit to a power-law global error model; differentially expressed proteins were then identified through a signal-to-noise (STN) test statistic. Proteins were kept for further analysis if spectra were detected in at least 2 samples per group or spectra were detected in all samples of one group and spectra were absent in all samples of the other group. The false discovery rate (FDR) was estimated by comparing the STN statistic to an empirically derived null distribution, using the resampling procedure described by Pavelka et al. and implemented in the ‘plgem’ R package (13).

*Preparation of tissue homogenates* – Control and septic hearts or other tissues (aorta, kidney, spleen, liver, lung, muscle, brain) were excised and washed briefly in ice-cold Tyrode`s solution (pH 7.4) containing in 130mmol/L NaCl, 5.4mmol/L KCl, 1.4mmol/L $MgCl_2$, 0.4mmol/L $NaH_2PO_4$, 4.2mmol/L HEPES to remove blood. The tissue was snap-frozen in liquid nitrogen, before homogenization using a motor driven blade `on ice` in a Tris-based homogenization buffer (pH 7.4) containing 100mmol/L Tris/HCl, 100mmol/L EDTA, 100mmol/L maleimide and protease inhibitors (Roche), at a ratio of 100mg/ml (10%). Laemmli sample buffer with 10% β-mercaptoethanol (reducing) or 100mmol/L maleimide (non-reducing) was added to the tissue homogenates and samples were passed through a narrow gauge needle to shear DNA.

*Preparation of mouse plasma samples* – Whole mouse blood from control or LPS-treated mice was collected and 2mmol/L EDTA was added. The samples were centrifuged for 15min at 2,000g at 4°C to deplete cells. Non-reducing Laemmli sample buffer was added to the resulting plasma supernatant.

*SDS-PAGE and immunoblot analysis* – Protein samples from tissue homogenates, fractionated homogenates or plasma samples in reducing or non-reducing Laemmli sample buffer were separated by 7.5, 10 or 15% SDS-PAGE, transferred to polyvinylidene difluoride (PVDF) membranes and subjected to immunoblotting. Primary antibodies were detected by donkey anti-rabbit or sheep anti-mouse secondary antibodies linked to horseradish peroxidase (HRP; GE Healthcare). Specific protein bands were detected by enhanced chemiluminescence (GE Healthcare) and quantified on a calibrated

densitometer (GS-800, BioRad) using Quantity One® 1-D analysis software (v-4.5.1).

*Fluorescence immunohistochemical staining* – Mouse hearts were prepared as described above. For antigen retrieval, deparaffinised sections were boiled for 60min in 10mM citrate buffer (10mM sodium citrate, 0.05% Tween20, pH 6.0) using a steamer. Afterwards, sections were blocked for 60 min in PBS containing donkey serum (1.2mg/ml; Dianova, Hamburg, Germany) followed by blocking with 1% Sudan black in 70% ethanol for 20min in order to decrease auto-fluorescence of the tissue. After rigorous washing, sections were incubated with anti-PTX3 (1:100; Epitomics, Abcam, Cambridge, UK) primary antibody overnight at 4°C. Sections were then washed again and secondary donkey anti-rabbit IgG Alexa 633 labelled antibody (1:200; Invitrogen, Darmstadt, Germany) was applied for 60min. Nuclei were counterstained by 0.4µg/ml 4'6-Diamidino-2'-phenylindole (DAPI; Roche, Munich, Germany) in PBS for 10min and slides were mounted in Fluoromount G (Biozol, Munich, Germany). Images were taken on a fluorescence light microscope equipped with a digital camera (Axio Imager M2, Zeiss, Jena, Germany).

*Study population* – An observational cohort study was performed in an 88-bed university hospital general medical-surgical intensive care unit (ICU). The study protocol received ethical approval from an Institutional Review Board (REC reference 12/LO/0326) and written informed consent was obtained either from the patient, if mentally competent, or from their next of kin and consent procedure completed with retrospective consent. The clinical management of the patient was at the discretion of the attending physicians.

The investigators analysing samples were blinded to the patient's outcome whilst conducting the experiments. Consecutive patients meeting the definition for severe sepsis within the first 12h following ICU admission between May - October 2011 were included. Severe sepsis was defined as evidence of two or more systemic inflammatory response syndrome (SIRS) criteria, with proven or suspected infection and at least one organ system dysfunction (cardiovascular, respiratory, renal, hematological or metabolic) (14). Organ function was classified and categorized using the sequential organ failure assessment (SOFA) score. Exclusion criteria included patients younger than 18yrs, those with congenital hypo-gammaglobulinemia, known protein-losing enteropathies, nephrotic syndrome, neoplastic or proliferative hematological diseases, those having received intravenous immunoglobulins (IVIg therapy) in the last 3 months, those receiving high dose steroid therapy, having other ongoing immune dysfunction as defined by the APACHE II co-morbidities, ongoing blood loss (defined by blood transfusion requirement > 2 units/ 24h period) and retroviral disease. Blood samples for measurements were obtained daily from day 0 (ICU admission) until day 6 and at day 11. Whole blood from septic patients was collected at the indicated time-points, the blood was allowed to clot by leaving it undisturbed at room-temperature for 15-30min. The clot was removed by centrifuging at 2000g for 10min at 4°C. Following centrifugation, the serum was immediately transferred into a clean polypropylene tube and stored at -80°C. For immunoblotting, serum samples were incubated with Blue Sepharose® CL-6B (50µl per 200µl serum) at 4°C for 1 h on a shaking platform to deplete from serum albumin. Samples were centrifuged at 1000g for 1min at 4°C to remove Blue Sepharose® CL-6B

beads, non-reducing Laemmli sample buffer was added, equal volumes of depleted samples were analysed by Western immunoblot analysis.

*Immunoassays* – NT-proBNP and hsTnT were determined by the electrochemiluminescence sandwich immunoassay ECLIA on an Elecsys 2010 system (Roche Diagnostics, Germany) in serum samples according to the manufacturers recommendations. The assay range for NT-proBNP was 5-35.000pg/mL, the assay range for hsTnT was 3-10.000pg/mL. HsTnI was determined by a cardiac troponin assay (ARCHITECT STAT highly sensitive Troponin I immunoassay, Abbott Diagnostics, USA, ARCHITECT i2000SR). The established limit of detection (LoD) for the assay ranges from 0.8-1.9 with a median of 1.5pg/mL and an assay range of 0-50.000pg/mL. Human Pentraxin 3/TSG-14 was measured in 28 participants, including all non-surivivors, by a Quantikine ELISA Kit from R&D Systems.

*Statistics* – Monomeric, tetrameric and octameric PTX3 levels in patients admitted to the ICU were not normally distributed. We therefore used the median and interquartile range to summarize their distributions and used the Wilcoxon rank-sum test to formally test for differences between participants who survived the 28-day follow-up period and those who did not. Analogous methods were used for the biomarkers NT-proBNP hsTnT and hsTnI. Analyses were performed using Stata release 12.1 (StataCorp, College Station, Texas). Statistical tests were two-sided and used a significance level of $P<0.05$.

## RESULTS

*Biomarker discovery in a pre-clincial model* - For our proteomic investigation, we chose the mouse model of endotoxemia to identify biomarker candidates. As a tissue susceptible to sepsis-induced dysfunction, hearts were isolated from control or septic mice 16-18h after injection of vehicle saline solution or lipopolysaccharide (LPS; 9mg/kg ip) (9). Before proteomics, all tissue specimen were examined histologically. Macrophage and neutrophil infiltration was detected by immunostaining within 6-8h after LPS injection. Representative images are shown in **Fig. 1A**. Hearts were obtained from four control and LPS-treated mice (n=4 per group). To enable a better characterization of inflammatory proteins retained within the cardiac tissue, we used a solubility-based protein subfractionation methodology based on 1% Triton. The Triton-insoluble protein extracts were separated by SDS-PAGE (**supplemental Fig. S1**), subjected to in-gel tryptic digestion and analyzed by liquid chromatography tandem mass spectrometry (LC-MS/MS) using a high mass accuracy ion trap (LTQ-Orbitrap XL, Thermo Fisher Scientific). The entire MS/MS dataset has been deposited to the ProteomeXchange Consortium via the PRIDE partner repository with the dataset identifier PXD001020 and DOI 10.6019/PXD001020 (http://www.ebi.ac.uk/pride/). Only proteins passing stringent identification criteria are listed in **supplemental Table S1** (n=1,910). The identified peptides corresponding to these protein identifications are given in **supplemental Table S2.** According to the Gene Ontology Annotation database 66 non-redundant proteins were secreted proteins in the Triton-insoluble fraction. Differences in relative protein abundance between control

and LPS-treated hearts were estimated using normalized spectral counts (**Table I**). No outliers were removed. Details can be found in *Experimental Procedures*. Long pentraxin 3 (PTX3) was returned as the most pronounced change (**Fig. 1B**). PTX3 is an acute phase glycoprotein, secreted in response to pro-inflammatory cytokines (15). The quantitative difference according to the proteomics data (**Fig. 1C**) was validated by immunoblotting. Immunblots confirmed a marked increase of PTX3 in the Triton-insoluble cardiac extracts under endotoxemic conditions (**Fig. 1D**). Equal protein loading was demonstrated by immunoblotting for the sarcomeric proteins α-actinin and cardiac myosin-binding protein C (cMyBP-C) and Coomassie staining.

*Redox-dependent oligomerisation of PTX3* - Oligomerization of PTX3 into tetrameric and octameric complexes via interprotein disulphide bond formation through adjacent cysteine residues in PTX3 monomer subunits was described as a prerequisite for its biological activity and binding to constituents of the extracellular matrix (16). To further investigate the enrichment of PTX3 in septic hearts, the Triton-soluble and Triton-insoluble fractions were compared under reducing as well as non-reducing conditions 6-8 h post LPS injection (n=3 per group). The effectiveness of the subfractionation procedure by 1% Triton was confirmed by immunoblotting for selected markers of different cardiomyocyte compartments, glyceraldehyde-3-phosphate dehydrogenase (GAPDH; cytosolic) and telethonin (particulate/myofilament) (**Fig. 2A**). Under reducing conditions, PTX3 was clearly detectable as a 45kDa moiety in sepsis hearts (**Fig. 2A,** upper panel). N-linked glycosylation accounts for a 5kDa shift of PTX3 with a predicted molecular mass for the reduced protein of 40kDa (17). Immunoblot analysis

performed under non-denaturing conditions revealed that PTX3 forms high molecular weight complexes resulting in the formation of tetramers (180 kDa) and octamers (360 kDa) (**Fig. 2A,** lower panel) in response to oxidant exposure. While both, the tetramer and the octamer were present in the Triton-soluble fraction, only the octamer was detectable in the Triton-insoluble fraction of septic hearts. Next, we tested different tissue homogenates. Interestingly, there was a preponderance of the oxidised versus the reduced form of PTX3 with oxidized PTX3 accumulating in the heart, aorta, kidney and lung - organs that are known to be susceptible to septic complications (**Fig. 2B,** upper and lower panel, respectively). Less oxidized PTX3 was retained in the spleen and liver. This is consistent with previous reports that LPS induces PTX3 expression *in vivo* in heart and lung but not in liver (18, 19). The high molecular weight PTX3 moieties were converted to monomers under reducing conditions. In contrast, no PTX3 protein was detectable in tissue homogenates of control mice. Notably, the immunoblots presented in **Fig. 2C** highlight bands consistent with the expected molecular weight of tetrameric and octameric moieties of PTX3 in plasma of septic mice. PTX3 can be expressed by a variety of cells in response to LPS and inflammatory cytokines (20, 21). Positive immunostaining for PTX3 in the heart was predominantly observed in the vicinity of smaller vessels (**Fig. 3**) at sites of leukocyte and macrophage infiltration (**supplemental Fig. S2**). Besides PTX3, known first and second degree interaction partners of PTX3 (www.innatedb.com) were identified in the proteomics screen (**Fig. 4**).

*Circulating PTX3 in sepsis patients* - PTX3 is barely detectable in plasma of healthy individuals (<2ng/ml) but increases up to 200ng/ml in

sepsis depending on the severity of the disease (22). High PTX3 plasma levels are correlated with severity of infection in patients with sepsis or septic shock (23-25). Based on our findings in the pre-clinical model, we quantified octameric, tetrameric and monomeric PTX3 levels in critically ill patients with sepsis but without established acute organ failure (AOF) referred to ICU Outreach Teams (n=31). Their clinical characteristics are shown in **Table II**. Samples were taken in a longitudinal manner at 8 different time points: on the day of admission to ICU (day 0), at days 1 to 6 and at day 11. Immunoblot analysis was performed under non-reducing conditions in a total of 204 samples (**Fig. 5A**). Next, we tested if the levels of the different oxidized PTX3 moieties can distinguish survivors from non-survivors. On day 0, there was no difference in octameric, tetrameric and monomeric PTX3 levels between survivors and non-survivors. Over the time course of 11 days, however, transformation of octameric to monomeric PTX3 was associated with a greater survival during 28 days follow-up (**Fig. 5B**). As early as day 2 post admission, PTX3 oxidation predicted adverse clinical outcome: Octameric PTX3 was barely detectable in survivors, but constituted more than 50% of total PTX3 in non-survivors ($p$<0.001, **Fig. 5C**). On the other hand, monomeric PTX3 constituted 90% of total PTX3 in survivors, but only 20% in non-survivors ($p$<0.013). There was no significant difference in tetrameric PTX3 between survivors and non-survivors.

*Comparison to established biomarkers* - Secreted PTX3 can bind to pathogens to induce classical complement activation (20). Notably, monomer levels of PTX3 were inversely correlated to complement C3a ($r_s$=-0.455, n=24,

p=0.014) as well as the cardiac and stress markers high sensitivity troponin I ($r_s$=-0.565, n=28, p=0.001), high sensitivity troponin T ($r_s$=-0.358, n=28, p=0.067) and N-terminal pro-B-type natriuretic peptide ($r_s$=-0.352, n=28, NT-proBNP, p=0.066) (**supplemental Fig. S3,** panel **A**), suggesting that the absence of oligomerisation is associated with less complement activation and less cardiac tissue damage. Patients with the maximum cardiovascular SOFA score (n=19) at day 1 post admission to ICU had on average 4-fold higher oligomerized PTX3 levels than patients with a lower cardiovascular SOFA score (n=12) (oligomerized PTX3, density in arbitrary units, mean±SEM: 1.38 ±0.40 vs 0.31±0.18, p=0.022). Unlike oxidized PTX3 moieties, the cardiac damage markers were not significantly correlated with the survival of patients (**supplemental Fig. S3,** panel **B**). Octameric- and monomeric-PTX3 levels at day 2 predicted the 28-day survival better than a model containing total PTX3 as measured by conventional ELISA (AUROC: 0.918 vs. 0.626; P value: 0.045, Fig. **Fig. 6A**) or NT-proBNP (AUROC: 0.918 vs. 0.687; P value: 0.023, **Fig. 6B**), a marker for left ventricular dysfunction that is frequently increased in severe sepsis (26). Although octameric to monomeric PTX3 was superior to total PTX3 and NT-proBNP, this single biomarker did not outperform the APACHE II score related risk prediction (AUROC 0.92 vs 0.80, p=0.25), which includes clinical variables, organ dysfunction biochemistry and accounts for co-morbidities (27).

## DISCUSSION

Our study provides proof-of-principle data that the oligomerization state of PTX3 may represent a superior prognostic marker than total PTX3 in adult critically ill patients with severe sepsis. This distinction between the oligomerization state of PTX3 compared to conventional measurements of total PTX3 is important, as the oligomerization state might better mirror the changes in the underlying complex interactions between immune-inflammatory insults and redox stress in sepsis. Furthermore, key strengths of our study are the bridging of proteomics discovery to bedside validation and the direct comparison to established biomarkers, which directly addresses the main criticisms often highlighted in proteomics biomarker research.

*Role of PTX3* - Together with CRP and serum amyloid P component, PTX3 belongs to the family of pentraxins. Although CRP is used as a marker of systemic inflammation, its prognostic value in sepsis is poor (28). PTX3 plays an important role in regulating the innate immune response by contributing to opsonisation (29). In mice, overexpression of PTX3 confers resistance to the lethal effects of LPS (30). LPS injection elicits the secretion of several cytokines, including interleukin-1 and tumor necrosis factor alpha, two potent inducers of PTX3. Unlike the classical pentraxins CRP and serum amyloid P component, PTX3 does not bind phosphoethanolamine or phosphocholine but collagen-like C1q, the first component of the classical pathway of complement activation. Its capacity to bind C1q is mediated by the pentraxin domain and requires multimer formation (17). Thus, PTX3 oligomers may better reflect activity than total PTX3 as measured by ELISA. As

expected on the basis of C1q binding, high PTX3 may cause the consumption of C4 and of the total complement hemolytic activity in serum (17).

*PTX3 and inflammation* - Resolution of inflammation is not a passive process but requires stop signals (31). In severe sepsis, an uncontrolled inflammatory response to infection causes damage to and subsequently failure of organs such as the lungs, heart and kidneys. The underlying mechanisms of AOF are not well understood and no effective mediator-targeted therapies of established AOF are available (32). Medical care of patients combines prompt treatment with antibiotics and supportive care and often requires artificial organ support provided in an ICU. Numerous studies have tested novel therapeutics attempting to block key steps in the inflammatory processes associated with AOF. However, despite over 200 sepsis randomised controlled trials since 1992, no effective therapies exist. Most interventions have failed when tested in rigorous trials (33). Previous anti-inflammatory interventions mainly targeted circulating inflammatory cells or inflammatory mediators, i.e. by dialysis. The observed retention of oxidized PTX3 in the Triton-insoluble fraction and the inverse correlation of monomeric plasma PTX3 with cardiac damage markers support the concept that inflammation and tissue damage may be perpetuated locally. Thus, in addition to targeting circulating mediators of inflammation, resolving the inflammation within the tissues might be a promising strategy in the prevention of AOF.

*Clinical significance* - AOF in sepsis is common, associated with high mortality, short-term morbidity, and significant chronic illness. Many biomarkers have been identified, but they lack specificity or sensitivity. Our tissue-based proteomics approach (34, 35) led to the novel observation that

the oligomerization state of PTX3 could be a better prognostic biomarker in sepsis than total PTX3 as measured by conventional ELISA. Mechanistically, PTX3 oxidation may be linked to innate immunity and increased oxidative stress during inflammation, i.e. by the respiratory burst during neutrophil extracellular trap formation. While levels of octameric PTX3 on admission day were not different between survivors and non-survivors, a dynamic change in the redox state of PTX3 within the first 2 days may assist to identify treatment response or lack of it in patients with progressive illness or persistent organ dysfunction. A single biomarker, however, is unlikley to outperform the APACHE Score, which consists of 12 variables (age, rectal temperature, mean arterial pressure, pH arterial, heart rate, respiratory rate, serum sodium, serum potassium, creatinine, haematocrit, leukocyte count as well as the Glasgow Coma Scale).

*Strengths and limitations* – ELISA technology is widely used in clinical diagnostics to detect total protein levels. In this study, we have demonstrated that the oligomerization state of circulating PTX3 may provide an important advantage over total PTX3 or cardiac damage markers in determining treatment response. Further studies in larger cohorts are required to confirm whether the oxidation state of PTX3 is a superior surrogate end point for therapeutic interventions. As a mediator molecule in the innate immune system responses, PTX3 multimers may not only be an indicator of but also a contributor towards the deleterious host responses in sepsis. Whether this is a mechanism for the prolongation of tissue inflammation and progression to AOF awaits clarification in future studies (36).

*Conclusions* - An estimated 200,000 US ICU patients die every year. Our findings suggest that the transformation of octameric to monomeric PTX3 in survivors may be a surrogate end point for the inflection point where oxidative stress subsides, and inflammation turns into resolution / repair. If sepsis patients at risk of developing AOF could be identified early, this novel biomarker could help to 'personalise' critical care medicine.

**Acknowledgements:** We thank Melanie Neumann and Kristin Hartmann (UKE HEXT core facility mouse pathology) for generating histology slides.

**Funding:** FC was supported by an RCUK Fellowship, the DZHK (German Center for Cardiovascular Research) and the German Ministry of Research and Education (BMBF). PW was supported by a British Heart Foundation PhD Studentship. MM is a Senior Fellow of the British Heart Foundation. The research was funded/supported by the National Institute of Health Research (NIHR) Biomedical Research Centre based at Guy's and St Thomas' NHS Foundation Trust and King's College London in partnership with King's College Hospital.

**Disclosures:** King's College has filed a patent application with regards to using oxidized PTX 3 as biomarker.

**REFERENCES**

1. Rittirsch, D., Flierl, M. A., and Ward, P. A. (2008) Harmful molecular mechanisms in sepsis. *Nat. Rev. Immunol.* **8**, 776-787

2. Anderson, N. L., and Anderson, N. G. (2002) The human plasma proteome: history, character, and diagnostic prospects. *Mol. Cell. Proteomics* **1**, 845-867

3. Anderson, L., and Hunter, C. L. (2006) Quantitative mass spectrometric multiple reaction monitoring assays for major plasma proteins. *Mol. Cell. Proteomics* **5**, 573-588

4. Jacquet, S., Yin, X., Sicard, P., Clark, J., Kanaganayagam, G. S., Mayr, M., and Marber, M. S. (2009) Identification of cardiac myosin-binding protein C as a candidate biomarker of myocardial infarction by proteomics analysis. *Mol. Cell. Proteomics* **8**, 2687-2699

5. Didangelos, A., Stegemann, C., and Mayr, M. (2012) The -omics era: proteomics and lipidomics in vascular research. *Atherosclerosis* **221**, 12-17

6. Mayr, M., Zampetaki, A., Willeit, P., Willeit, J., and Kiechl, S. (2013) MicroRNAs within the continuum of postgenomics biomarker discovery. *Arterioscl. Thromb. Vasc. Biol.* **33**, 206-214

7. Mayr, M., Zhang, J., Greene, A. S., Gutterman, D., Perloff, J., and Ping, P. (2006) Proteomics-based development of biomarkers in cardiovascular disease: mechanistic, clinical, and therapeutic insights. *Mol. Cell. Proteomics* **5**, 1853-1864

8. Abi-Gerges, N., Tavernier, B., Mebazaa, A., Faivre, V., Paqueron, X., Payen, D., Fischmeister, R., and Mery, P-F. (1999) Sequential changes in autonomic regulation of cardiac myocytes after in vivo endotoxin injection in rats. *Am. J. Resp. Crit. Care Med.* **160**, 1196–120

9. Tavernier, B., Li, J. M., El-Omar, M. M., Lanone, S., Yang, Z. K., Trayer, I. P., Mebazaa, A., and Shah, A. M. (2001) Cardiac contractile impairment associated with increased phosphorylation of troponin I in endotoxemic rats. *FASEB.* **15**, 294-296

10. Yin, X., Bern, M., Xing, Q., Ho, J., Viner, R., and Mayr, M. (2013) Glycoproteomic analysis of the secretome of human endothelial cells. *Mol. Cell. Proteomics* **12**, 956-78

11. Yin, X., Cuello, F., Mayr, U., Hao, Z., Hornshaw, M., Ehler, E., Avkiran, M., and Mayr, M. (2010) Proteomics analysis of the cardiac myofilament

subproteome reveals dynamic alterations in phosphatase subunit distribution. *Mol. Cell. Proteomics* **9**, 497-509

12. Pavelka, N., Fournier, M. L., Swanson, S. K., Pelizzola, M., Ricciardi-Castagnoli, P., Florens, L., and Washburn, M. P. (2008) Statistical similarities between transcriptomics and quantitative shotgun proteomics data. *Mol. Cell. Proteomics* **7**, 631-644

13. Pavelka, N., Pelizzola, M., Vizzardelli, C., Capozzoli, M., Splendiani, A., Granucci, F. and Ricciardi-Castagnoli, P. (2004) A power law global error model for the identification of differentially expressed genes in microarray data. *BMC Bioinformatics*, **5**:203

14. Levy, M. M., Fink, M. P., Marshall, J. C., Abraham, E., Angus, D., Cook, D., Cohen, J., Opal, S. M., Vincent, J. L., and Ramsay, G. (2003) 2001 SCCM/ESICM/ACCP/ATS/SIS International Sepsis Definitions Conference. *Crit. Care Med.* **31**, 1250-1256

15. Bottazzi, B., Doni, A., Garlanda, C., and Mantovani, A. (2010) An integrated view of humoral innate immunity: pentraxins as a paradigm. *Annu. Rev. Immunol.* **28**, 157-183

16. Inforzato, A., Rivieccio, V., Morreale, A. P., Bastone, A., Salustri, A., Scarchilli, L., Verdoliva, A., Vincenti, S., Gallo, G., Chiapparino, C., Pacello, L., Nucera, E., Serlupi-Crescenzi, O., Day, A. J., Bottazzi, B., Mantovani, A., De Santis, R., and Salvatori, G. (2008) Structural characterization of PTX3 disulfide bond network and its multimeric status in cumulus matrix organization. *J. Biol. Chem.* **283**, 10147-10161

17. Bottazzi, B., Vouret-Craviari, V., Bastone, A., De Gioia, L., Matteucci, C., Peri, G., Spreafico, F., Pausa, M., D'Ettorre, C., Gianazza, E., Tagliabue, A., Salmona, M., Tedesco, F., Introna, M., and Mantovani, A. (1997) Multimer formation and ligand recognition by the long pentraxin PTX3. Similarities and differences with the short pentraxins C-reactive protein and serum amyloid P component. *J. Biol. Chem.* **272**, 32817-32823

18. Introna, M., Alles, V. V., Castellano, M., Picardi, G., De Gioia, L., Bottazzai, B., Peri, G., Breviario, F., Salmona, M., De Gregorio, L., Dragani, T. A., Srinivasan, N., Blundell, T. L., Hamilton, T. A., and Mantovani, A. (1996) Cloning of mouse ptx3, a new member of the pentraxin gene family expressed at extrahepatic sites. *Blood* **87**, 1862-1872

19. Lee, G. W., Goodman, A. R., Lee, T. H., and Vilcek, J. (1994) Relationship of TSG-14 protein to the pentraxin family of major acute phase proteins. *J. Immunol.* **153**, 3700-3707

20. Alles, V. V., Bottazzi, B., Peri, G., Golay, J., Introna, M., and Mantovani, A. (1994) Inducible expression of PTX3, a new member of the pentraxin family, in human mononuclear phagocytes. *Blood* **84**, 3483-3493

21. Breviario, F., d'Aniello, E. M., Golay, J., Peri, G., Bottazzi, B., Bairoch, A., Saccone, S., Marzella, R., Predazzi, V., Rocchi, M., and et al. (1992) Interleukin-1-inducible genes in endothelial cells. Cloning of a new gene related to C-reactive protein and serum amyloid P component. *J. Biol. Chem.* **267**, 22190-22197

22. Daigo, K., Yamaguchi, N., Kawamura, T., Matsubara, K., Jiang, S., Ohashi, R., Sudou, Y., Kodama, T., Naito, M., Inoue, K., and Hamakubo, T. (2012) The proteomic profile of circulating pentraxin 3 (PTX3) complex in sepsis demonstrates the interaction with azurocidin 1 and other components of neutrophil extracellular traps. *Mol. Cell. Proteomics* **11**, M111 015073

23. Huttunen, R., and Aittoniemi, J. (2011) New concepts in the pathogenesis, diagnosis and treatment of bacteremia and sepsis. *J. Infect.* **63**, 407-419

24. Mauri, T., Bellani, G., Patroniti, N., Coppadoro, A., Peri, G., Cuccovillo, I., Cugno, M., Iapichino, G., Gattinoni, L., Pesenti, A., and Mantovani, A. (2010) Persisting high levels of plasma pentraxin 3 over the first days after severe sepsis and septic shock onset are associated with mortality. *Intensive Care Med.* **36**, 621-629

25. Uusitalo-Seppala, R., Huttunen, R., Aittoniemi, J., Koskinen, P., Leino, A., Vahlberg, T., and Rintala, E. M. (2013) Pentraxin 3 (PTX3) is associated with severe sepsis and fatal disease in emergency room patients with suspected infection: a prospective cohort study. *PloS one* **8**, e53661

26. Wang, F., Wu, Y., Tang, L., Zhu, W., Chen, F., Xu, T., Bo, L., Li, J., and Deng, X. (2012) Brain natriuretic peptide for prediction of mortality in patients with sepsis: a systematic review and meta-analysis. *Crit. Care* **16**, R74

27. Knaus, W.A., Draper, E.A., Wagner, D.P., and Zimmerman, J.E. (1985) APACHE II: a severity of disease classification system. *Crit. Care. Med*. **13**, 818-29.

28. Silvestre, J., Povoa, P., Coelho, L., Almeida, E., Moreira, P., Fernandes, A., Mealha, R., and Sabino, H. (2009) Is C-reactive protein a good prognostic marker in septic patients? *Intensive Care Med.* **35**, 909-913

29. Bottazzi, B., Garlanda, C., Cotena, A., Moalli, F., Jaillon, S., Deban, L., and Mantovani, A. (2009) The long pentraxin PTX3 as a prototypic humoral pattern recognition receptor: interplay with cellular innate immunity. *Immunol. Rev.* **227**, 9-18

30. Dias, A. A., Goodman, A. R., Dos Santos, J. L., Gomes, R. N., Altmeyer, A., Bozza, P. T., Horta, M. F., Vilcek, J., and Reis, L. F. (2001) TSG-14 transgenic mice have improved survival to endotoxemia and to CLP-induced sepsis. *J. Leukoc. Biol.* **69**, 928-936

31. Li, Y., Dalli, J., Chiang, N., Baron, R. M., Quintana, C., and Serhan, C. N. (2013) Plasticity of leukocytic exudates in resolving acute inflammation is regulated by microRNA and proresolving mediators. *Immunity* **39**, 885-898

32. Marshall, J. C. (2003) Such stuff as dreams are made on: mediator-directed therapy in sepsis. *Nat. Rev. Drug. Discov.* **2**, 391-405

33. Sweeney, D. A., Danner, R. L., Eichacker, P. Q., and Natanson, C. (2008) Once is not enough: clinical trials in sepsis. *Intensive Care Med.* **34**, 1955-1960.

34. Didangelos, A., Yin, X., Mandal, K., Baumert, M., Jahangiri, M., and Mayr, M. (2010) Proteomics characterization of extracellular space components in the human aorta. *Mol Cell Proteomics.* **9**, 2048-62

35. Didangelos, A., Yin, X., Mandal, K., Saje, A., Smith, A., Xu, Q., Jahangiri, M., and Mayr, M. (2011) Extracellular matrix composition and remodeling in human abdominal aortic aneurysms: a proteomics approach. *Mol Cell Proteomics.* **10**, M111.008128.

36. Thiele, J. R., Habersberger, J., Braig, D., Schmidt, Y., Goerendt, K., Maurer, V., Bannasch, H., Scheichl, A., Woollard, K., von Dobschütz, E., Kolodgie, F., Virmani, R., Stark, G. B., Peter, K, and Eisenhardt, S. U. (2014). The dissociation of pentameric to monomeric C-Reactive protein localizes and aggravates Inflammation: In vivo proof of a powerful pro-Inflammatory mechanism and a new anti-Inflammatory strategy. *Circulation.* published online before print, doi:10.1161/CIRCULATIONAHA.113.007124

**FIGURE LEGENDS**

**Figure 1. Proteomics in a pre-clinical model of sepsis. A,** Hematoxylin and eosin (H/E) staining of hearts from control C57Bl6 and LPS-treated mice. Immunostaining for the macrophage marker ionized calcium binding adaptor molecule 1 (Iba1) and the granulocyte marker Ly6G. **B**, Differential expression in the proteomic analysis. Note the pronounced upregulation of pentraxin 3 (PTX3) in the Triton-insoluble fraction of LPS-treated hearts. **C**, Comparative quantification for PTX3 by mass spectrometry; Equal expression of $\alpha$-actinin-1 (ACTN1_MOUSE) and cardiac myosin-binding protein C (MYPC3_MOUSE); **D**, Representative immunoblots of the Triton-insoluble fraction performed on 4 hearts per group. Probing for $\alpha$-actinin; cardiac myosin-binding protein C (cMyBP-C); and Coomassie staining assured equal protein loading.

**Figure 2. Redox state of PTX3 in endotoxemia. A,** The different oxidation states of PTX3 in the heart (octamer, tetramer and monomer) were visualized in the triton-soluble (sol) and insoluble (insol) fractions under reducing (upper panel) or non-reducing conditions (bottom panel). Representative immunoblots from 3 mouse hearts per group were probed for PTX3, telethonin (marker of the insoluble myofilament containing compartment) and GAPDH (marker of the soluble cytosol containing compartment). **B,** Tissue samples from heart, aorta, kidney, spleen, liver, lung, muscle and brain were subjected to immunoblot analysis under non-reducing (upper panel) or reducing (bottom panel) gel conditions and probed for PTX3. **C,** Plasma samples from control C57Bl6 and LPS-treated mice were depleted of albumin and analysed for PTX3 protein content and oxidation state using immunoblot

analysis under non-reducing conditions. The representative immunoblots display the results of 4 mice per group.

**Figure 3. Localization of PTX3.** Immunofluorescence staining for PTX3. Perivascular localization of PTX3 (green) in hearts from LPS-treated mice. Nuclear counter-staining with DAPI (blue).

**Figure 4. Protein interactions of PTX3.** Protein interactions of PTX3, from Innate DB (www.innatedb.com), are shown with PTX3 in red. The dark grey nodes are the second-degree interaction proteins from PTX3; the light grey nodes are proteins that form a complex, which interacts with PTX3. Abbreviations are given as Gene ID (Human). The large nodes in blue are proteins identified by proteomics (**supplemental Table S1**).

**Figure 5. Association of PTX3 oligomerization with patient survival. A,** Representative immunoblots of the development of the PTX3 oligomerization state with time after admission in a non-surviving sepsis patient (upper panel) compared to a surviving sepsis patient (bottom panel). N-numbers corresponding to patient death or dropout are given for each time point. **B,** Serum samples from 31 septic patients after admission to ICU (day 0) over a time course of 11 days were analysed for PTX3 levels after albumin depletion. Monomeric, tetrameric and octameric PTX3 levels were quantified for each patient and time point using Western immunoblot analysis performed under non-reducing conditions. * Denotes statistical significant difference between patients who died and those who survived during follow-up time (28 days);

P<0.05. **C,** Distribution of PTX3 oxidation levels on day 2 post admission to ICU compared between survivors and non-survivors.

**Figure 6. Comparison of the discriminatory power of octameric- and monomeric-PTX3 and other markers. A,** ROC curves of PTX3 measurements compared to total PTX3. Octameric and monomeric PTX3 levels at day 2 predicted the 28-day survival better than a model containing total PTX3 as measured by conventional ELISA (28 observations, areas under the ROC (AUROC): 0.918 vs. 0.626; P value: 0.045). **B,** ROC curves of PTX3 measurements compared to NT-proBNP and the clinical APACHE II score. Octameric and monomeric PTX3 levels at day 2 predicted the 28-day survival better than a model containing NT-proBNP (28 observations, AUROC: 0.918 vs. 0.687; P value: 0.023) but failed to significantly outperform the APACHE II score in this patient cohort (28 observations, AUROC: 0.918 vs. 0.803, p=0.25).

**Table I:** Extracellular/secreted proteins identified by proteomics in the Triton-insoluble fraction of cardiac tissue.

[a] Four biological samples analysed per group (n = 4);
* Indicates proteins with a False Discovery Rate (FDR) ≤ 0.1.

| Protein name | SwissProt Accession | Control[a] (Mean spectra ±SD) | LPS[a] (Mean spectra±SD) | log Fold change | FDR |
|---|---|---|---|---|---|
| Pentraxin-related protein PTX3 | PTX3_MOUSE | 0±0 | 10±4 | 19.67 | 0.003* |
| Galectin-1 | LEG1_MOUSE | 8±3 | 22±4 | 1.36 | 0.016* |
| Thioredoxin | THIO_MOUSE | 4±5 | 9±5 | 1.02 | 0.049* |
| von Willebrand factor A domain-containing protein 1 | VWA1_MOUSE | 6±1 | 2±2 | -1.71 | 0.058* |
| Versican | CSPG2_MOUSE | 8±16 | 1±1 | -3.14 | 0.062* |
| Inter alpha-trypsin inhibitor heavy chain 4 | ITIH4_MOUSE | 3±3 | 9±7 | 1.51 | 0.078* |
| Vitronectin | VTNC_MOUSE | 4±3 | 8±7 | 1.15 | 0.094* |
| Complement C3 | CO3_MOUSE | 2±2 | 6±4 | 1.64 | 0.109 |
| Mimecan | MIME_MOUSE | 5±2 | 2±2 | -1.12 | 0.112 |
| Prolargin | PRELP_MOUSE | 18±12 | 29±10 | 0.66 | 0.117 |
| Antithrombin-III | ANT3_MOUSE | 2±1 | 4±3 | 1.12 | 0.135 |
| Calmodulin | CALM_MOUSE | 3±4 | 5±5 | 0.73 | 0.14 |
| Reticulon-3 | RTN3_MOUSE | 4±2 | 2±2 | -1.38 | 0.14 |
| Complement C1q tumor necrosis factor related protein 9 | C1QT9_MOUSE | 4±4 | 2±2 | -0.98 | 0.161 |
| Dermatopontin | DERM_MOUSE | 23±6 | 16±4 | -0.49 | 0.169 |
| Collagen alpha-1 (I) | CO1A1_MOUSE | 6±7 | 3±4 | -1.09 | 0.194 |
| Laminin subunit beta-2 | LAMB2_MOUSE | 54±8 | 35±14 | -0.60 | 0.211 |
| Collagen alpha-6 (VI) | CO6A6_MOUSE | 2±2 | 5±2 | 1.09 | 0.238 |
| Dystroglycan | DAG1_MOUSE | 5±1 | 3±2 | -0.84 | 0.248 |
| Uncharacterized aarF domain containing protein kinase 1 | ADCK1_MOUSE | 1±1 | 2±2 | 0.91 | 0.256 |
| Annexin A2 | ANXA2_MOUSE | 8±2 | 12±3 | 0.47 | 0.257 |
| Laminin subunit alpha-5 | LAMA5_MOUSE | 4±2 | 1±2 | -1.31 | 0.264 |
| Collagen alpha-1 (XV) | COFA1_MOUSE | 15±2 | 10±3 | -0.66 | 0.265 |
| Apolipoprotein A-I | APOA1_MOUSE | 6±3 | 4±3 | -0.49 | 0.295 |
| Vinculin | VINC_MOUSE | 131±52 | 106±8 | -0.30 | 0.309 |
| Translationally-controlled tumor protein | TCTP_MOUSE | 3±4 | 2±3 | -0.48 | 0.323 |
| Decorin | PGS2_MOUSE | 25±10 | 30±6 | 0.28 | 0.346 |
| Inter-alpha trypsin inhibitor heavy chain 1 | ITIH1_MOUSE | 6±2 | 9±3 | 0.48 | 0.356 |
| Periostin | POSTN_MOUSE | 11±6 | 15±6 | 0.40 | 0.367 |
| Fibrinogen gamma chain | FIBG_MOUSE | 6±3 | 8±4 | 0.39 | 0.371 |
| Cadherin-13 | CAD13_MOUSE | 19±5 | 15±3 | -0.36 | 0.382 |
| Clusterin | CLUS_MOUSE | 3±1 | 4±4 | 0.44 | 0.396 |
| Papilin | PPN_MOUSE | 16±7 | 12±4 | -0.43 | 0.396 |
| Perlecan | PGBM_MOUSE | 10±4 | 7±3 | -0.56 | 0.439 |
| Ceruloplasmin | CERU_MOUSE | 3±1 | 4±3 | 0.45 | 0.452 |

| | | | | | |
|---|---|---|---|---|---|
| Peroxidasin homolog | PXDN_MOUSE | 5±4 | 7±4 | 0.44 | 0.452 |
| Glutathione peroxidase 3 | GPX3_MOUSE | 5±5 | 6±2 | 0.27 | 0.456 |
| Protein-glutamine gamma-glutamyltransferase 2 | TGM2_MOUSE | 27±2 | 31±11 | 0.23 | 0.466 |
| Collagen alpha-1 (VI) | CO6A1_MOUSE | 84±13 | 73±22 | -0.20 | 0.481 |
| Galectin-9 | LEG9_MOUSE | 4±1 | 3±3 | -0.34 | 0.482 |
| EMILIN-1 | EMIL1_MOUSE | 15±5 | 12±4 | -0.31 | 0.492 |
| EGF-containing fibulin-like extracellular matrix protein 1 | FBLN3_MOUSE | 4±2 | 3±2 | -0.37 | 0.492 |
| Coatomer subunit alpha | COPA_MOUSE | 2±2 | 2±3 | 0.49 | 0.497 |
| Talin-1 | TLN1_MOUSE | 10±3 | 7±6 | -0.38 | 0.537 |
| Nidogen-1 | NID1_MOUSE | 88±16 | 78±8 | -0.17 | 0.543 |
| Filamin-A | FLNA_MOUSE | 8±7 | 6±2 | -0.39 | 0.546 |
| Apolipoprotein O | APOO_MOUSE | 13±6 | 12±6 | -0.17 | 0.558 |
| Dehydrogenase/reductase SDR family member 7C | DRS7C_MOUSE | 21±5 | 18±5 | -0.17 | 0.558 |
| Gelsolin | GELS_MOUSE | 5±2 | 4±2 | -0.29 | 0.565 |
| Fibronectin | FINC_MOUSE | 2±1 | 3±2 | 0.41 | 0.574 |
| Apolipoprotein O-like | APOOL_MOUSE | 23±8 | 25±11 | 0.13 | 0.588 |
| von Willebrand factor A domain-containing protein 8 | VWA8_MOUSE | 14±3 | 12±9 | -0.25 | 0.608 |
| Asporin | ASPN_MOUSE | 5±5 | 5±3 | -0.15 | 0.687 |
| Collagen alpha-2 (VI) | CO6A2_MOUSE | 47±4 | 44±10 | -0.10 | 0.708 |
| Laminin subunit gamma-1 | LAMC1_MOUSE | 35±12 | 32±4 | -0.12 | 0.721 |
| Protein disulfide-isomerase | PDIA1_MOUSE | 2±2 | 3±1 | 0.16 | 0.721 |
| Transforming growth factor-beta-induced protein ig-h3 | BGH3_MOUSE | 9±3 | 10±1 | 0.12 | 0.721 |
| Nidogen-2 | NID2_MOUSE | 10±7 | 10±3 | 0.13 | 0.74 |
| Lumican | LUM_MOUSE | 26±8 | 28±9 | 0.06 | 0.764 |
| Tubulointerstitial nephritis antigen-like | TINAL_MOUSE | 10±4 | 11±4 | 0.08 | 0.767 |
| Fibulin-5 | FBLN5_MOUSE | 2±3 | 3±2 | 0.11 | 0.779 |
| Laminin subunit beta-1 | LAMB1_MOUSE | 22±8 | 23±6 | 0.08 | 0.789 |
| Plasminogen | PLMN_MOUSE | 2±2 | 1±0 | -0.10 | 0.842 |
| Fibromodulin | FMOD_MOUSE | 2±3 | 2±3 | 0.06 | 0.845 |
| Fibrinogen beta chain | FIBB_MOUSE | 6±4 | 6±2 | 0.02 | 0.882 |
| Matrin-3 | MATR3_MOUSE | 8±3 | 8±3 | -0.02 | 0.913 |
| Laminin subunit alpha-2 | LAMA2_MOUSE | 46±10 | 46±7 | 0.00 | 0.924 |

**Table II.** Clinical Characteristics of Sepsis Patients

| Variable* | Entire Study cohort (n=31) | 28 day Survivors (n=23) | 28 day Non-Survivors (n=8) | p-value† |
|---|---|---|---|---|
| Age (years) | 67.4±11.9 | 66 .0±12.2 | 71.0±12.8 | 0.29 |
| Male: Female, n (%) | 19:12 (61.3%:38.3%) | 15:8 (65.3%:34.7%) | 4:4 (50.0%:50.0%) | 0.45 |
| APACHE II Score | 20.6±6.0 | 19.3±6.1 | 24.4±3.7 | 0.03 |
| Medical: Surgical, n | 26:5 (83.8%:16.1%) | 18:5 (78.3%:21.7%) | 8 (100%) | 0.20 |
| WCC (x $10^9$ / L) | 13.5 (1.3, 49.1) | 11.3 (1.3,25.8) | 17.8 (11.8, 49.1) | 0.04 |
| CRP (mg / L) | 130 (8,429) | 143 (8,429) | 115 (29,148) | 0.13 |
| CVS SOFA score | 4 (0,4) | 4 (0,4) | 4 (0,4) | 0.47 |
| Renal SOFA score | 1 (0,4) | 1 (0,4) | 0 (0,4) | 0.50 |
| t-SOFA score | 8 (4,12) | 8 (2,14) | 8 (3,13) | 0.98 |
| RRT, n | 5 | 4 | 1 | 0.77 |
| ICU LOS (days) | 9.9±5.7 | 9.5±6.3 | 11±3.5 | 0.23 |
| Hospital LOS (days) | 23 (4,216) | 30 (7,216) | 11 (4,18) | 0.001 |

APACHE: Acute Physiology and Chronic Health Evaluation II; WCC: white cell count; CRP: C-reactive protein; CVS SOFA: cardiovascular sequential organ failure assessment; t-SOFA: Total sequential organ failure assessment (t-SOFA); RRT: renal replacement therapy; LOS: length of stay.

* Values presented are unadjusted means ±SD, range (min,max) or percentages.

† P-values were calculated with the t-Test (continuous variables) or the Chi2-Test (categorical variables).

Figure 1

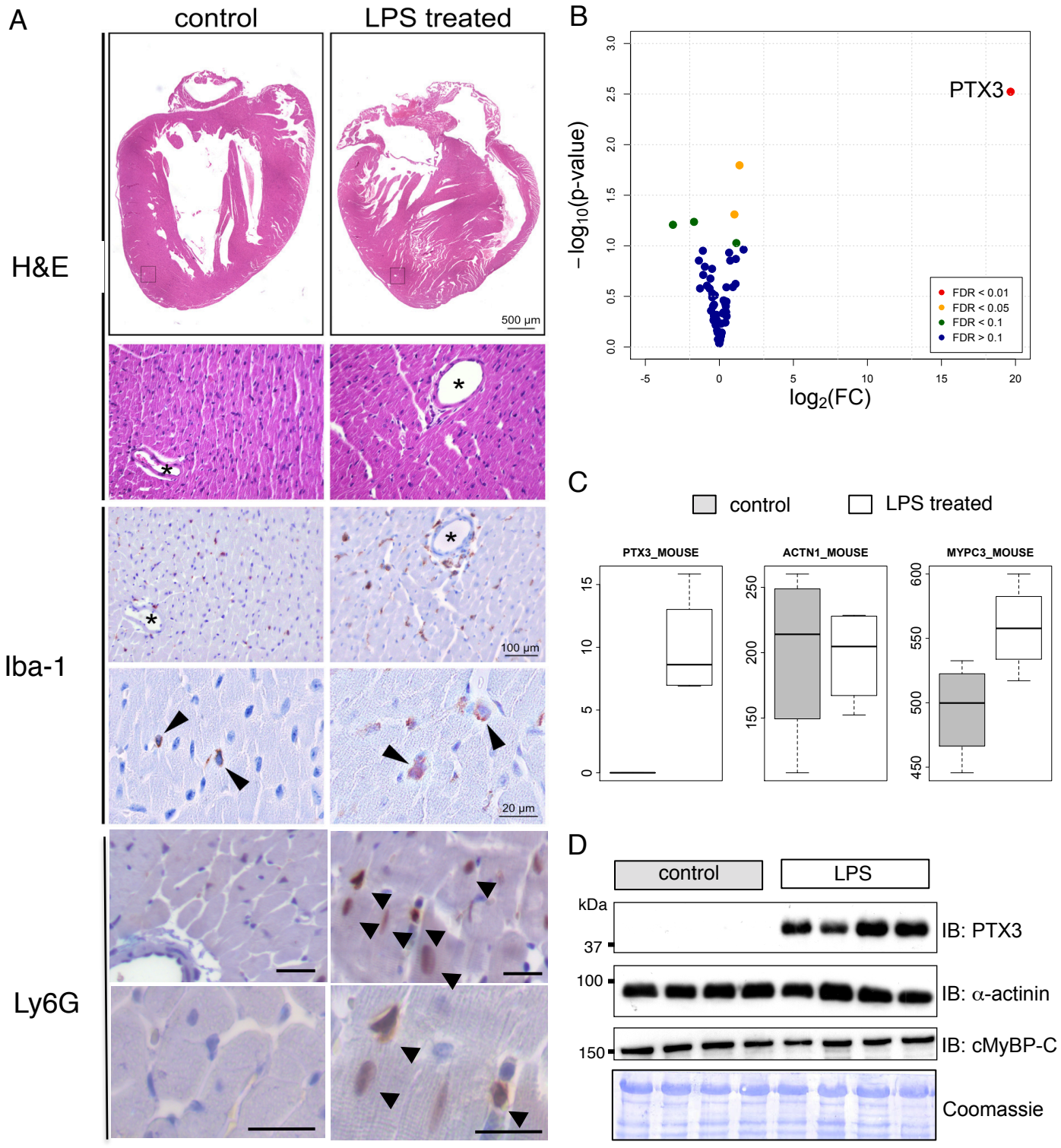
A
control
LPS treated
H&E
500 µm
Iba-1
100 µm
20 µm
Ly6G
B
PTX3
$-\log_{10}$(p-value)
$\log_2$(FC)
FDR < 0.01
FDR < 0.05
FDR < 0.1
FDR > 0.1
C
control
LPS treated
PTX3_MOUSE
ACTN1_MOUSE
MYPC3_MOUSE
D
control
LPS
kDa
37
100
150
IB: PTX3
IB: α-actinin
IB: cMyBP-C
Coomassie

Figure 2

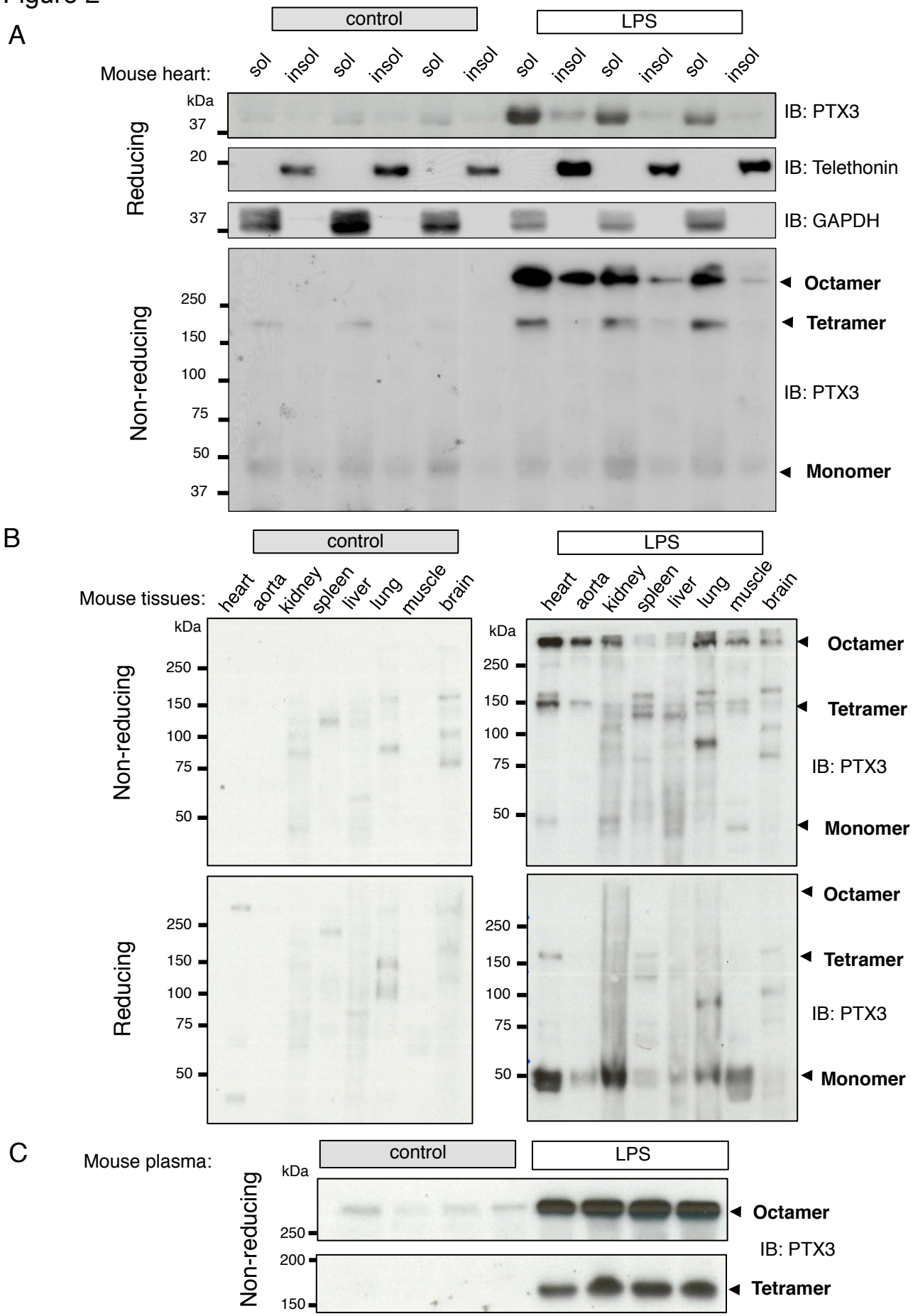
A
control
LPS
Mouse heart:
sol
insol
kDa
Reducing
37
20
IB: PTX3
IB: Telethonin
IB: GAPDH
Non-reducing
250
150
100
75
50
Octamer
Tetramer
Monomer
B
Mouse tissues:
heart
aorta
kidney
spleen
liver
lung
muscle
brain
C
Mouse plasma:
200

Figure 3

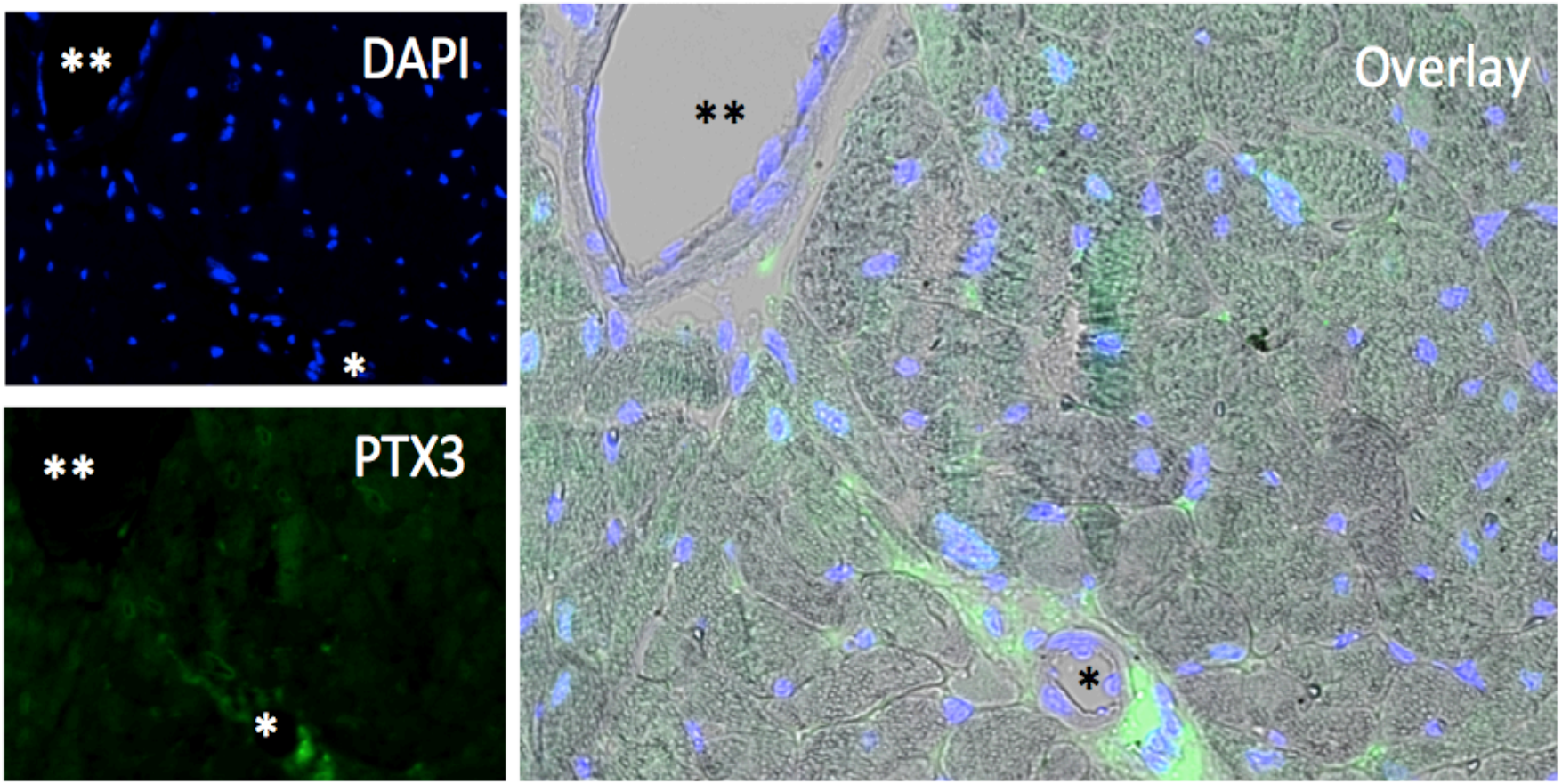

Figure 4

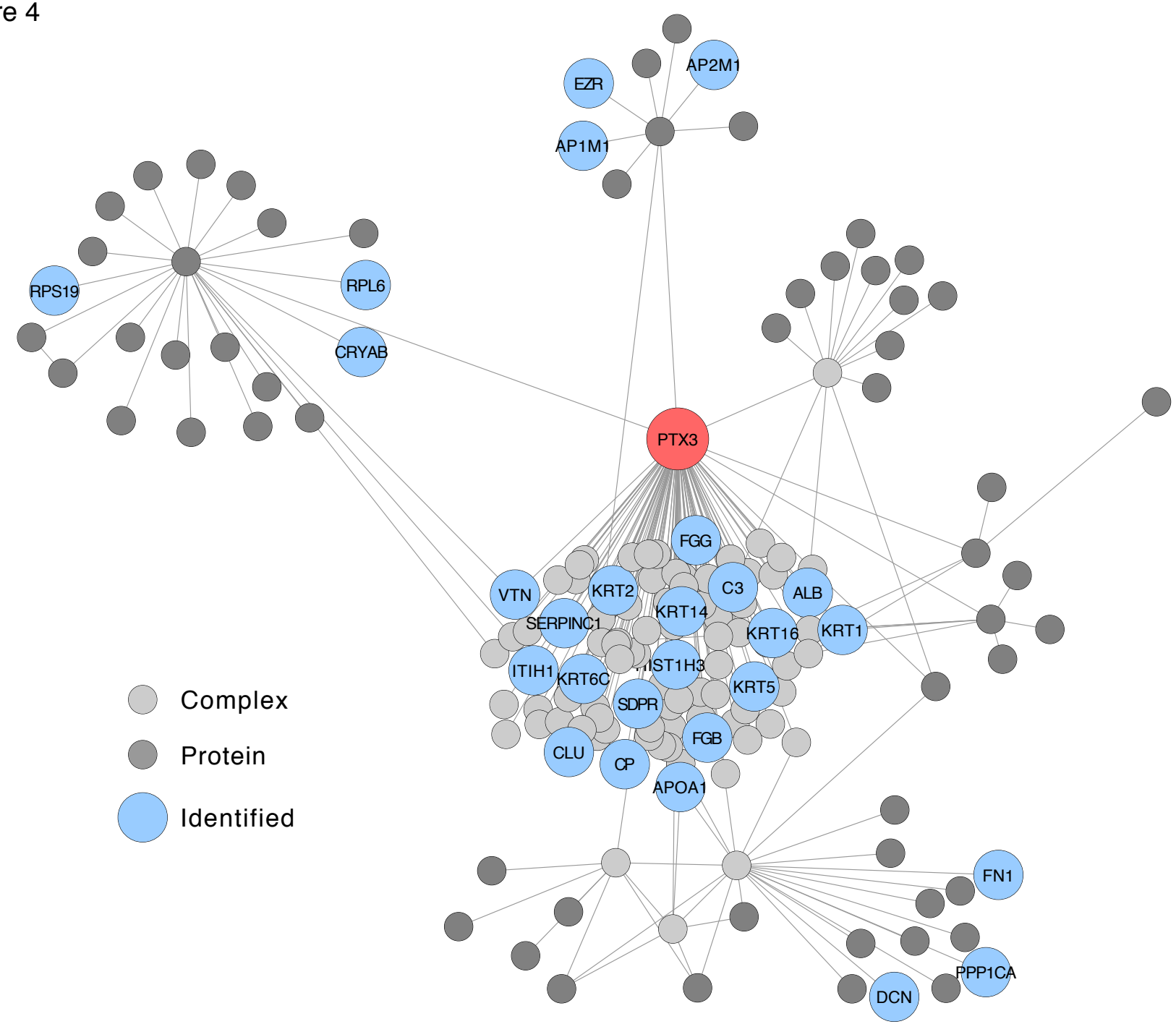
AP2M1
EZR
AP1M1
RPS19
RPL6
CRYAB
PTX3
FGG
VTN
KRT2
C3
ALB
SERPINC1
KRT14
KRT16
KRT1
ITIH1
KRT6C
HIST1H3
KRT5
SDPR
FGB
CLU
CP
APOA1
FN1
PPP1CA
DCN
Complex
Protein
Identified

Figure 5

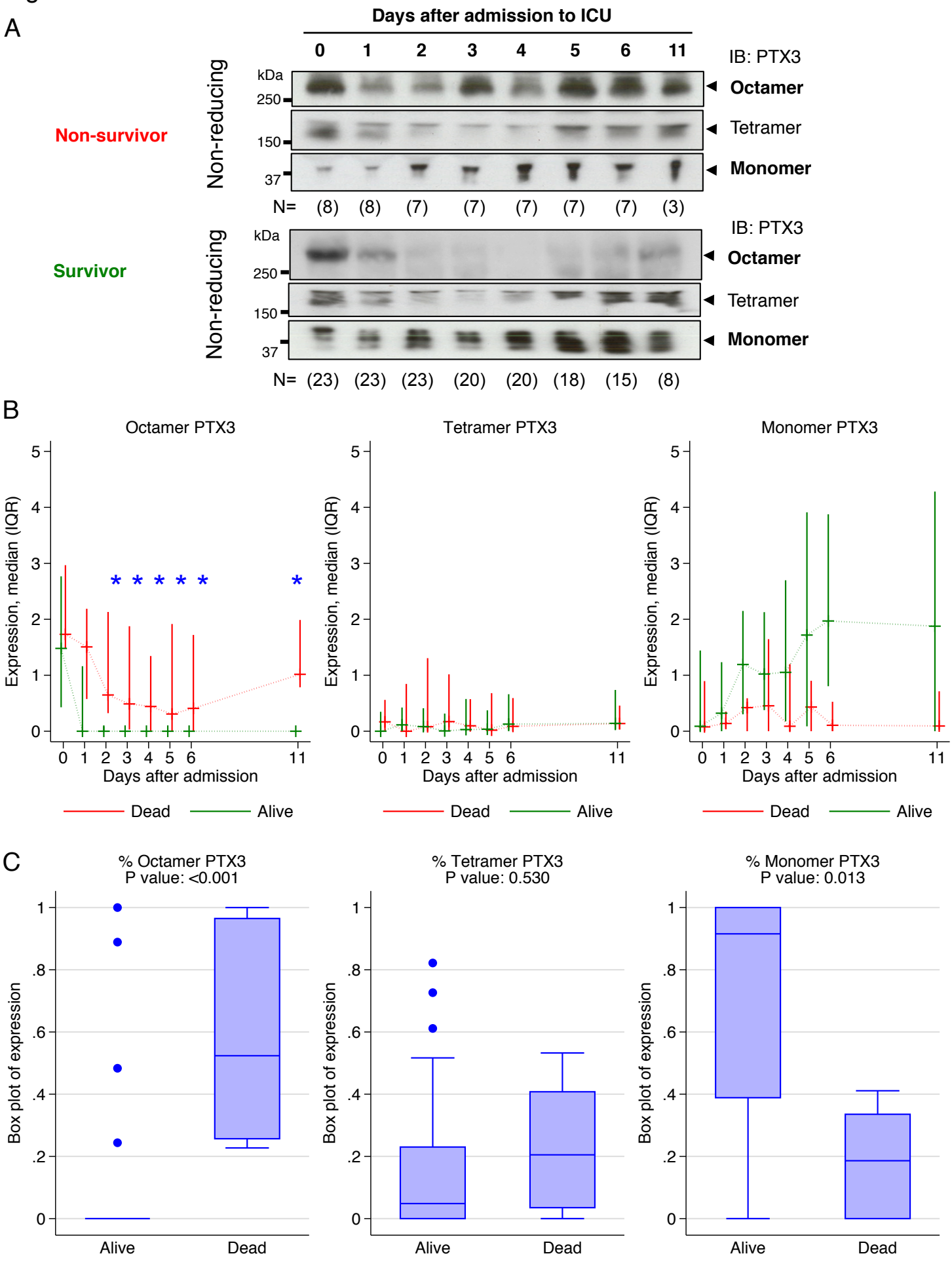
A
Days after admission to ICU
0 1 2 3 4 5 6 11
IB: PTX3
Non-survivor
Non-reducing
kDa
250
150
37
Octamer
Tetramer
Monomer
N= (8) (8) (7) (7) (7) (7) (7) (3)
Survivor
Non-reducing
IB: PTX3
Octamer
Tetramer
Monomer
N= (23) (23) (23) (20) (20) (18) (15) (8)
B
Octamer PTX3
Tetramer PTX3
Monomer PTX3
Expression, median (IQR)
Days after admission
Dead
Alive
C
% Octamer PTX3
P value: <0.001
% Tetramer PTX3
P value: 0.530
% Monomer PTX3
P value: 0.013
Box plot of expression
Alive
Dead

Figure 6

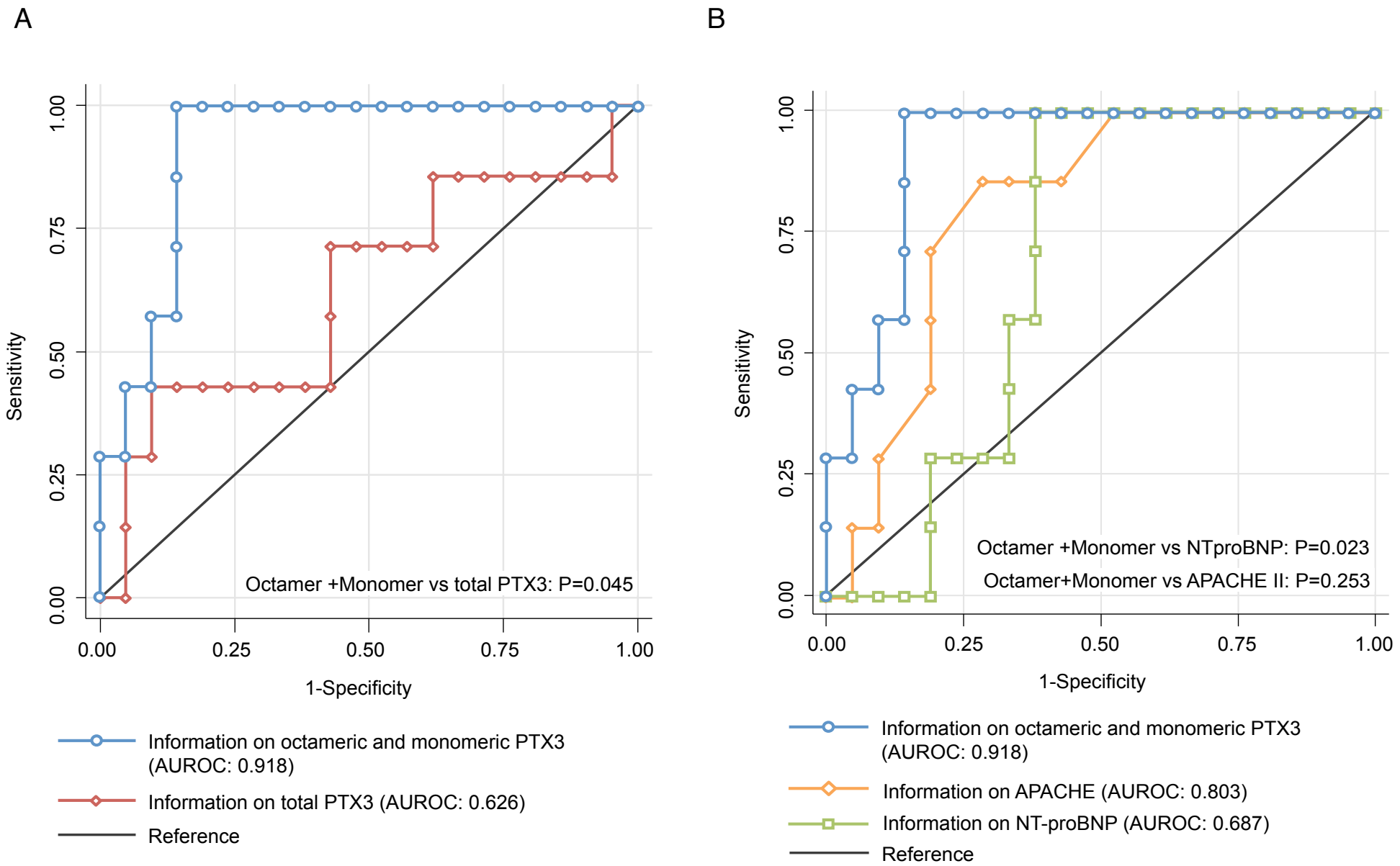
A
B
Sensitivity
1-Specificity
0.00
0.25
0.50
0.75
1.00
Octamer +Monomer vs total PTX3: P=0.045
Octamer +Monomer vs NTproBNP: P=0.023
Octamer+Monomer vs APACHE II: P=0.253
Information on octameric and monomeric PTX3 (AUROC: 0.918)
Information on total PTX3 (AUROC: 0.626)
Reference
Information on APACHE (AUROC: 0.803)
Information on NT-proBNP (AUROC: 0.687)